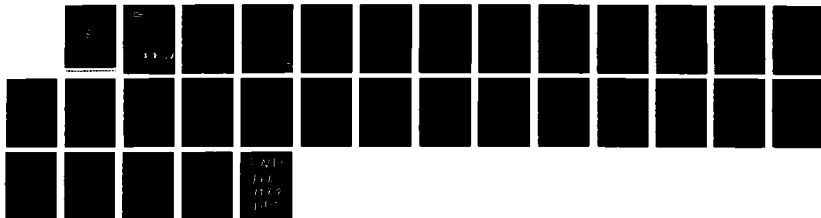
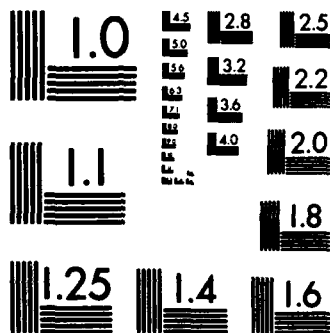


AD-A187 871

CHRISTIANSEN EFFECT IN INFRARED SPECTRA OF SOIL-DERIVED 1/1  
ATMOSPHERIC DUSTS(U) CHEMICAL RESEARCH DEVELOPMENT AND  
ENGINEERING CENTER ABERDEEN H R CARLON SEP 87  
CRDEC-TR-87069 F/G 4/1 NL

UNCLASSIFIED





MICROCOPY RESOLUTION TEST CHART  
NATIONAL BUREAU OF STANDARDS-1963-A

DTIC FILE COPY

**CHEMICAL  
RESEARCH,  
DEVELOPMENT &  
ENGINEERING  
CENTER**

CRDEC-TR-87069

AD-A187 071

**CHRISTIANSEN EFFECT IN INFRARED SPECTRA  
OF SOIL-DERIVED ATMOSPHERIC DUSTS**

by **Hugh R. Carlon**  
**RESEARCH DIRECTORATE**

September 1987

**DTIC**  
**ELECTE**  
**S** **D**  
DEC 03 1987  
H



**U.S. ARMY  
ARMAMENT  
MUNITIONS  
CHEMICAL COMMAND**

Aberdeen Proving Ground, Maryland 21010-5423

**DISTRIBUTION STATEMENT A**  
Approved for public release;  
Distribution Unlimited

**Disclaimer**

The findings in this report are not to be construed as an official Department of the Army position unless so designated by other authorizing documents.

**Distribution Statement**

Approved for public release; distribution is unlimited.

UNCLASSIFIED

SECURITY CLASSIFICATION OF THIS PAGE

REPORT DOCUMENTATION PAGE

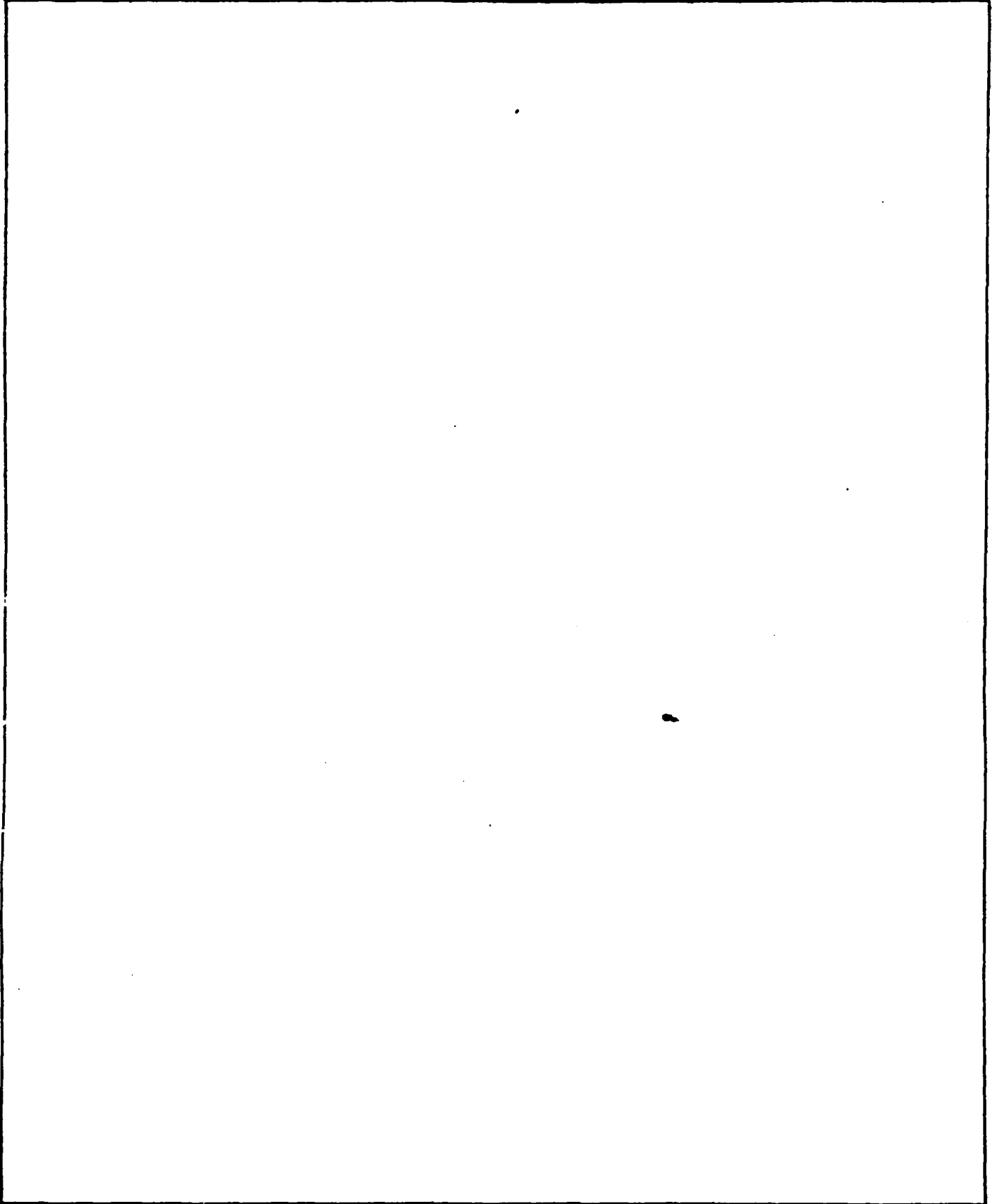
1a. REPORT SECURITY CLASSIFICATION <b>UNCLASSIFIED</b>		1b. RESTRICTIVE MARKINGS <b>AD-A187071</b>	
2a. SECURITY CLASSIFICATION AUTHORITY		3. DISTRIBUTION / AVAILABILITY OF REPORT Approved for public release; distribution is unlimited.	
2b. DECLASSIFICATION / DOWNGRADING SCHEDULE			
4. PERFORMING ORGANIZATION REPORT NUMBER(S) CRDEC-TR-87069		5. MONITORING ORGANIZATION REPORT NUMBER(S)	
6a. NAME OF PERFORMING ORGANIZATION CRDEC	6b. OFFICE SYMBOL (If applicable) SMOCR-RSP-P	7a. NAME OF MONITORING ORGANIZATION	
6c. ADDRESS (City, State, and ZIP Code) Aberdeen Proving Ground, MD 21010-5423		7b. ADDRESS (City, State, and ZIP Code)	
8a. NAME OF FUNDING / SPONSORING ORGANIZATION CRDEC	8b. OFFICE SYMBOL (If applicable) SMOCR-RSP-P	9. PROCUREMENT INSTRUMENT IDENTIFICATION NUMBER	
8c. ADDRESS (City, State, and ZIP Code) Aberdeen Proving Ground, MD 21010-5423		10. SOURCE OF FUNDING NUMBERS	
		PROGRAM ELEMENT NO.	PROJECT NO. 1L161101
		TASK NO. A91A	WORK UNIT ACCESSION NO.
11. TITLE (Include Security Classification) Christiansen Effect in Infrared Spectra of Soil-Derived Atmospheric Dusts			
12. PERSONAL AUTHOR(S) Carlton, Hugh R.			
13a. TYPE OF REPORT Technical	13b. TIME COVERED FROM 79 Jan TO 82 Dec	14. DATE OF REPORT (Year, Month, Day) 1987 September	15. PAGE COUNT 28
16. SUPPLEMENTARY NOTATION			
17. COSATI CODES		18. SUBJECT TERMS (Continue on reverse if necessary and identify by block number)	
FIELD	GROUP	Christiansen Effect Atmosphere Aerosols	
07	04	Refractive Index Infrared Dusts	
20	06	Optical Bandpass Suspensions	
19. ABSTRACT (Continue on reverse if necessary and identify by block number) The Christiansen effect occurs when a suspension of particles in a transparent medium is observed at a wavelength where the refractive indices of the particles and of the medium are equal, thus producing an optically homogeneous medium with optical bandpass or filter characteristics. It is shown that soil-derived atmospheric dusts and other particulates can exhibit the Christiansen effect at IR wavelengths and that their spectra can be simulated by equivalent, precipitated films of the particulates on optical substrates. Useful approximation equations are given. The implication of these observations should be considered by atmospheric physicists and IR system designers.			
20. DISTRIBUTION / AVAILABILITY OF ABSTRACT <input checked="" type="checkbox"/> UNCLASSIFIED/UNLIMITED <input type="checkbox"/> SAME AS RPT. <input type="checkbox"/> DTIC USERS		21. ABSTRACT SECURITY CLASSIFICATION <b>UNCLASSIFIED</b>	
22a. NAME OF RESPONSIBLE INDIVIDUAL TIMOTHY E. HAMPTON		22b. TELEPHONE (Include Area Code) (301) 671-2914	22c. OFFICE SYMBOL SMOCR-SPS-T



Special  
A-1

UNCLASSIFIED

SECURITY CLASSIFICATION OF THIS PAGE



UNCLASSIFIED

SECURITY CLASSIFICATION OF THIS PAGE

## PREFACE

The work described in this report was authorized under Project No. 1L161101A91A, Independent Laboratory In-House Research (ILIR) and performed between January 1979 and December 1982.

The use of trade names or manufacturers' names in this report does not constitute an official endorsement of any commercial products. This report may not be cited for purposes of advertisement.

Reproduction of this document in whole or in part is prohibited except with permission of the Commander, U.S. Army Chemical Research, Development and Engineering Center, ATTN: SMCCR-SPS-T, Aberdeen Proving Ground, Maryland 21010-5423. However, the Defense Technical Information Center is authorized to reproduce the document for U.S. Government purposes.

This report has been approved for release to the public.

Blank

## CONTENTS

	Page
1. INTRODUCTION . . . . .	7
1.1 General . . . . .	7
1.2 Definitions . . . . .	8
2. THEORY . . . . .	8
3. EXPERIMENTAL PROCEDURES . . . . .	15
4. DISCUSSION . . . . .	17
5. CONCLUSIONS . . . . .	20
LITERATURE CITED . . . . .	21
APPENDIX: ADDITIONAL OBSERVATIONS . . . . .	23

## LIST OF FIGURES

	Page
1. Dispersion of Silica (Quartz) for Ordinary Ray . .	9
2. Transmission of Quartz Powder Films, 12.8- $\mu$ m Layer Thickness, Three Different Particle Sizes . . .	10
3. Transmission of Quartz Powder Films, 15.5- $\mu$ m Particle Size . . . . .	11
4. Curves Showing the Christiansen Transmission Peaks for Powdered KCl, KBr, and KI . . . . .	13
5. Shift of the Christiansen Peak for Quartz Powder in Liquids. (a) Quartz in a 50% by Volume Mixture of CS <sub>2</sub> and CCl <sub>4</sub> ; (b) Quartz in Pure CCl <sub>4</sub> ; (c) Quartz in Air . . . . .	14
6. Measured IR Spectrum of an Experimental Dust Cloud and Calculated Spectra for Longer Optical Path Lengths or Cloud Depths . . . . .	16

Blank

# CHRISTIANSEN EFFECT IN INFRARED SPECTRA OF SOIL-DERIVED ATMOSPHERIC DUSTS

## 1. INTRODUCTION

### 1.1 General.

The well-known Christiansen effect<sup>1,2</sup> occurs when a suspension of particles in a transparent medium is observed at a wavelength  $\lambda$  where the refractive indices of the particles and of the medium are equal, thus producing an optically homogeneous medium. The particles scatter (or absorb) radiation at other wavelengths. The optical bandpass of the medium thus obtained depends upon the optical constants and size distributions of the particles, and upon the slopes of the refractive index curves, for the particles and for the transparent medium, at the Christiansen wavelength where these curves intersect.

An atmospheric aerosol is a suspension of particles in a medium that is transparent in the window regions where other atmospheric constituents do not absorb radiation, e.g., in the IR at 3-5  $\mu\text{m}$  and 7-13  $\mu\text{m}$ . Thus, if wavelengths could be found where the refractive indices of the particles and of the medium (essentially air, with a refractive index  $n_\lambda \approx 1.0$ ) were equal, a Christiansen filter with bandpass characteristics would be formed by the aerosol. Further, it has been shown previously<sup>3</sup> that liquid aerosol clouds can be simulated in some circumstances by precipitated liquid films of equivalent thickness. It will be shown in this report that such techniques also are possible for aerosols of solid particles, including soil-derived dust clouds, and are, in fact, conventional for Christiansen filters formed by powders in air on optical substrates. Thus, it is possible to represent an atmospheric dust cloud by an equivalent precipitated layer or film of dust particles having the same size distribution as the cloud. If the precipitated film exhibits the Christiansen effect at some wavelength, the atmospheric dust cloud will exhibit it at this wavelength also. Interest in filters of this kind has existed at this laboratory for many years. The original work was concerned with IR transmission filters fabricated from powdered mineral dusts or thin polyethylene substrates in air.<sup>4</sup> An extensive bibliography on the Christiansen effect has been researched and published by Reichert.<sup>5</sup>

An interesting example of the Christiansen effect occurs near 7.4  $\mu\text{m}$ , on the lower-wavelength edge of the 7-13  $\mu\text{m}$  IR atmospheric window, for powdered quartz (silica) particles in air. Silica and related compounds including silicates, are major constituents of soil-derived atmospheric dusts.<sup>6</sup> Thus, if precipitated films of silica dust in air can be shown to exhibit the Christiansen effect, atmospheric clouds of silica dusts could also exhibit this effect, with enhanced optical

transmittance near 7.4  $\mu\text{m}$  compared to other wavelengths, because of the optical bandpass characteristics of such dusts in the air. This report explores the possibility that such wavelengths may be favored for optical transmission and that they may thus be optimum wavelengths for design of new laser systems. The Appendix contains additional observations and applications.

## 1.2 Definitions.

- $a_\lambda$  = optical extinction coefficient at wavelength  $\lambda$ ,  $\text{m}^2/\text{g}$ .  
 $C$  = aerosol particle mass concentration,  $\text{g}/\text{m}^3$ .  
 $D_\mu$  = aerosol particle diameter or geometric mean diameter,  $\mu\text{m}$ .  
 $K_\lambda$  = imaginary part of the complex index of refraction  $(n - ik)_\lambda$ , at wavelength  $\lambda$ , unitless.  
 $k_{L_\lambda}, k^1_{L_\lambda}$  = absorption coefficient of an equivalent precipitated film or layer, for ordinary or extraordinary ray, respectively,  $\mu\text{m}^{-1}$ .  
 $L$  = optical path length, meters (m).  
 $\lambda$  = wavelength,  $\mu\text{m}$ .  
 $n_\lambda$  = real part of the complex index of refraction  $(n - ik)_\lambda$  at wavelength  $\lambda$ , unitless.  
 $p$  = density,  $\text{g}/\text{cm}^3$ .  
 $t$  = thickness of an equivalent precipitated film or layer,  $\mu\text{m}$ .  
 $T_\lambda$  = optical transmittance at wavelength  $\lambda$ , unitless.

## 2. THEORY

Figure 1 shows the variation of the real index of refraction of silica  $n_\lambda$  with wavelength, i.e., its dispersion, for an ordinary ray.<sup>7</sup> The Christiansen wavelength can be seen at  $\lambda = 7.4 \mu\text{m}$ , where  $n_{7.4} \approx 1.0$ , and silica particles thus have the same refractive index as air. Since the silica particles are transparent (i.e., have little absorption or a small imaginary refractive index  $k_\lambda$  at this wavelength), the medium becomes optically homogeneous, no scattering occurs, and a high optical transmittance results.

Detailed studies of silica (quartz) dust films were made by Henry,<sup>8</sup> who experimented with films of different particle sizes and thicknesses. Figure 2 shows his results for a quartz dust film 12.8  $\mu\text{m}$  thick, where particle diameters of  $D_\mu = 1.0 \mu\text{m}$ , 6.6  $\mu\text{m}$ , and 15.5  $\mu\text{m}$  were investigated. Figure 3 shows Henry's results for quartz particles where  $D_\mu = 15.5 \mu\text{m}$  and filter thicknesses of 4.1  $\mu\text{m}$ , 6.7  $\mu\text{m}$ , and 14.9  $\mu\text{m}$  were used. It is possible for a particle diameter to exceed the equivalent film. This technique is not unlike that reported more recently for liquid droplet aerosols.<sup>3</sup> However, it is important to realize that for dusts, Henry's technique is merely a computational convenience.

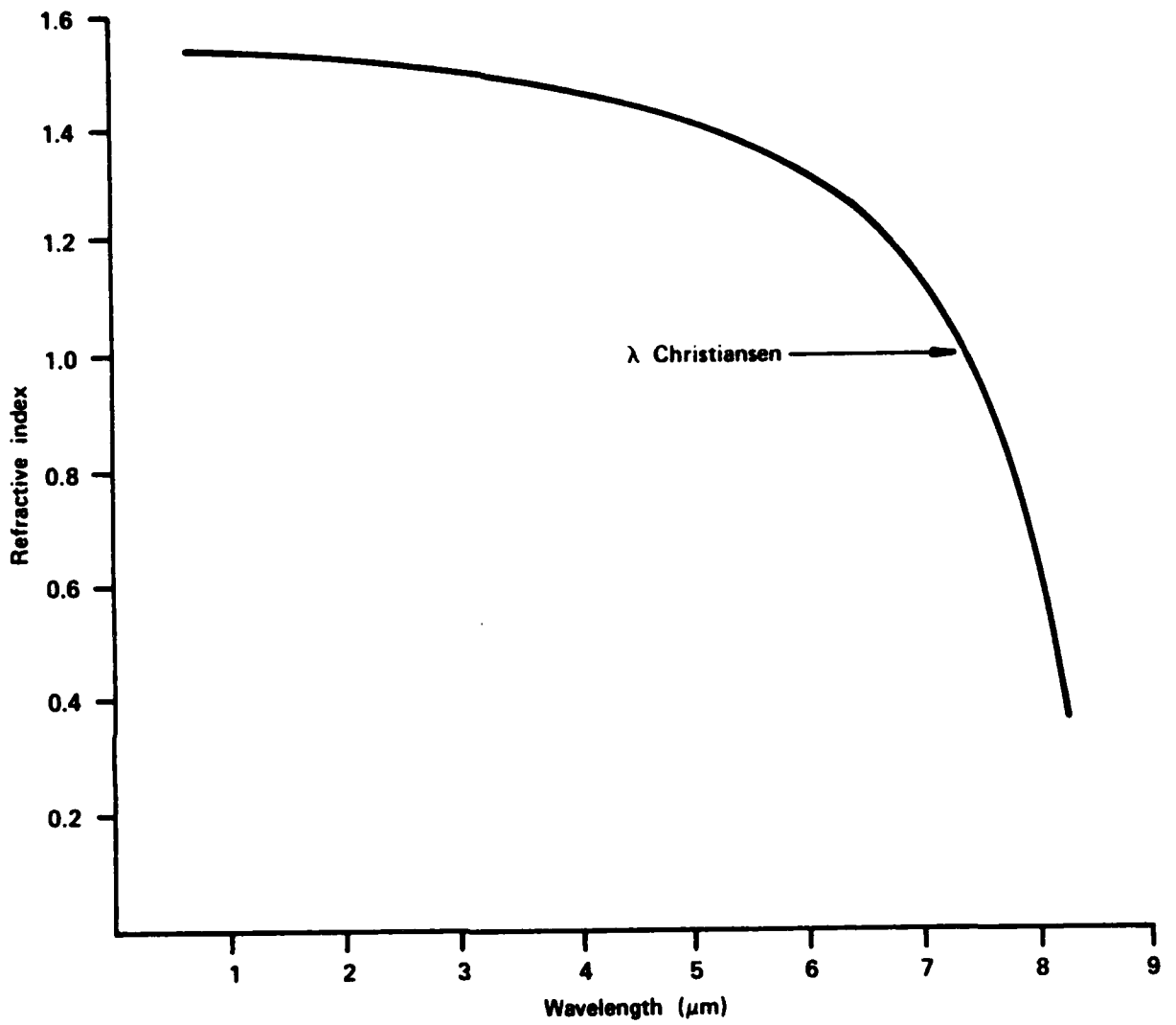


Figure 1. Dispersion of Silica (Quartz) for Ordinary Ray.

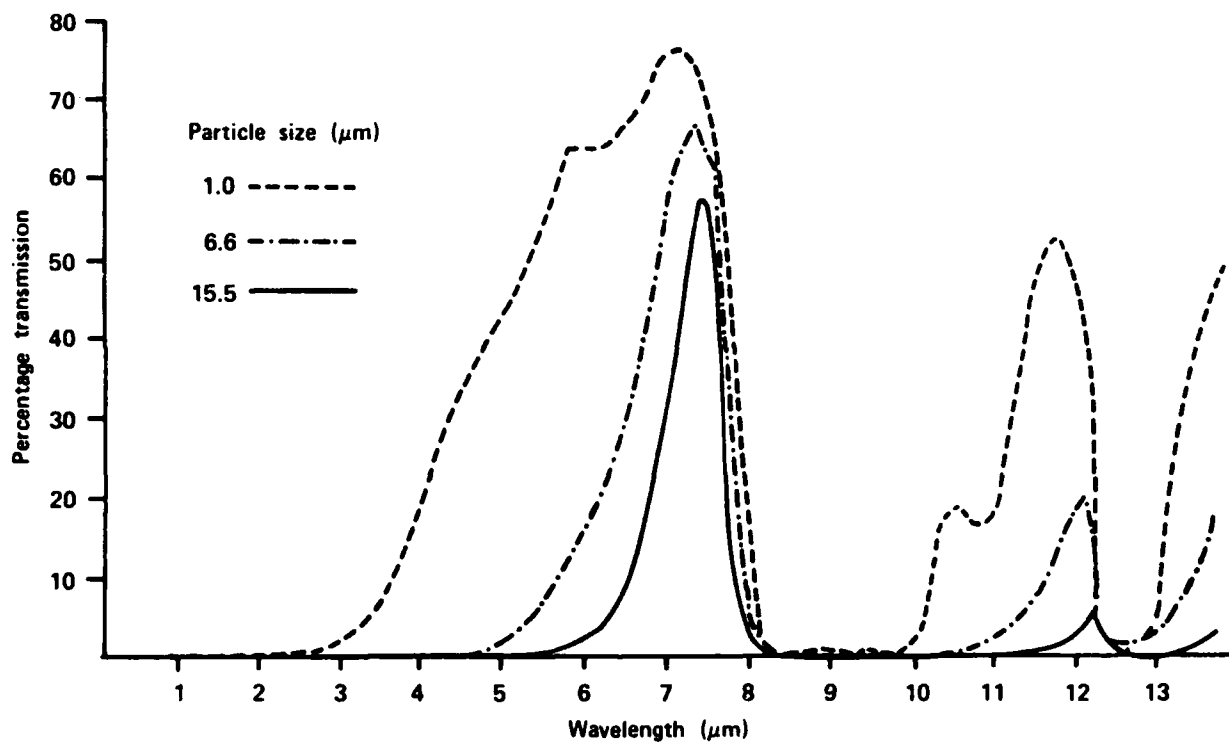


Figure 2. Transmission of Quartz Powder Films, 12.8- $\mu\text{m}$  Layer Thickness, Three Different Particle Sizes<sup>8</sup>

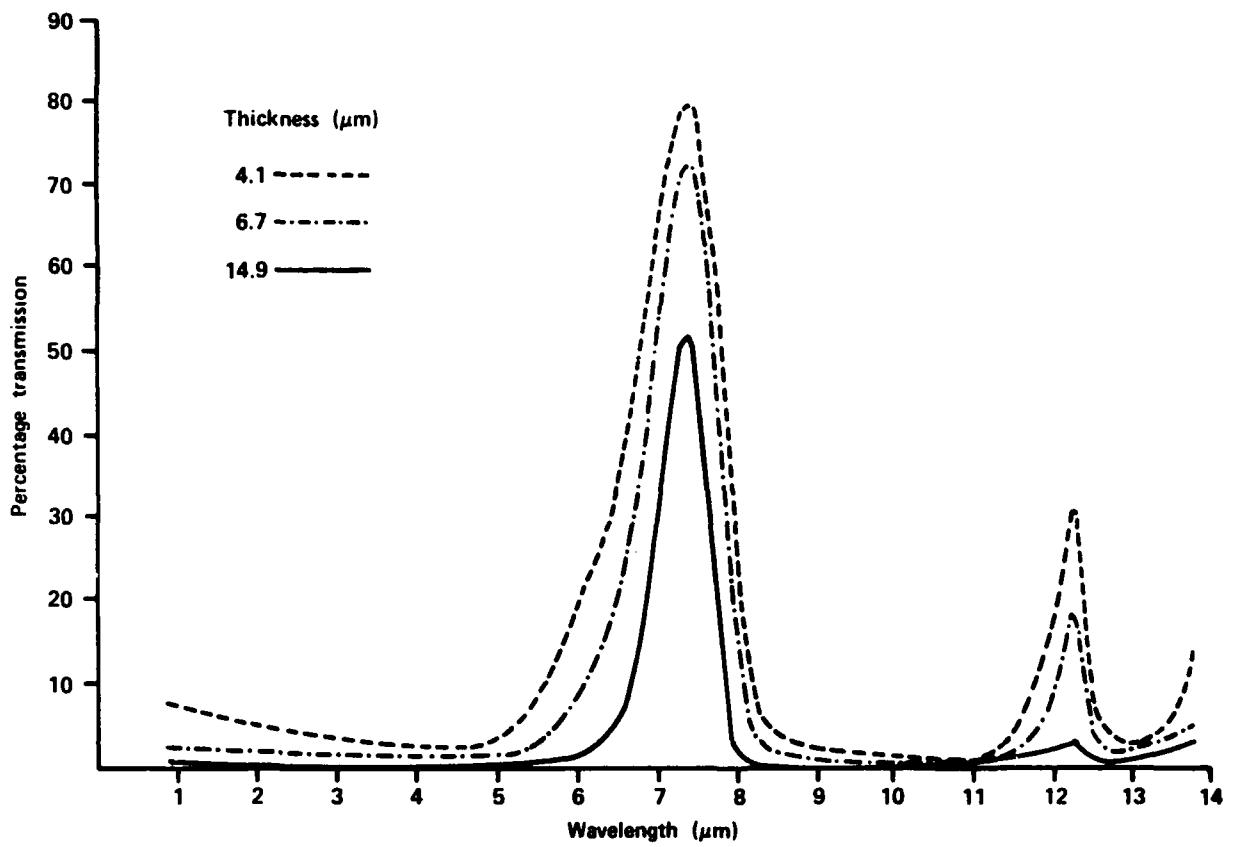


Figure 3. Transmission of Quartz Powder Films, 15.5- $\mu\text{m}$  Particle Size<sup>8</sup>

When it occurs, the Christiansen effect appears to be the same whether the dusts are dispersed as particulate clouds or are precipitated on substrates. This is probably due to the irregular shapes of dust particles, which minimize surface contact area between adjoining particles, even when they are loosely packed on a substrate. Figure 2 seems to indicate, from the range of  $D_p$  values, that a cloud of silica dust in air should have a relatively high transmittance (small extinction) near  $\lambda = 7.5 \mu\text{m}$  even if the particle size distribution were quite broad.<sup>6</sup> Henry also noted<sup>8</sup> that the transmission peak near  $12 \mu\text{m}$  in Figure 2 is Christiansenlike. Although refractive indices given by Henry for quartz do not drop to  $n_{12} = 1.0$ , data of other workers<sup>9</sup> indicate that a value of unity may be reached to make a Christiansen effect possible.

Besides silica, other powdered minerals in air give Christiansen transmission peaks at other wavelengths, as is shown in Table 1 and in Figure 4. The Christiansen effect, of course, is not limited to the special case of solid particles, like dusts in air or in other gases. For comparison, Figure 5 shows curves for silica powders in liquids and air. The optical passbands that result are quite sharp and occur at widely different wavelengths, depending upon the selected medium. These curves suggest the interesting possibility that aerosols of solid particles imbedded in liquid droplets, or in other solids, might be potentially useful at Christiansen wavelengths for special applications. For example, some of the wavelengths in the figures and in Table 1 should be available using isotopic gas laser technology already in existence.

Table 1. Christiansen Wavelengths of Various Powdered Minerals in Air

Mineral (dust)	Christiansen wavelength ( $\mu\text{m}$ )
Silica-SiO <sub>2</sub> (quartz)	7.4
LiF	11.2
MgO	12.2
NaCl	32
NaBr	37
NaI	49
KBr	52
KI	64
RbI	73
TlI	90

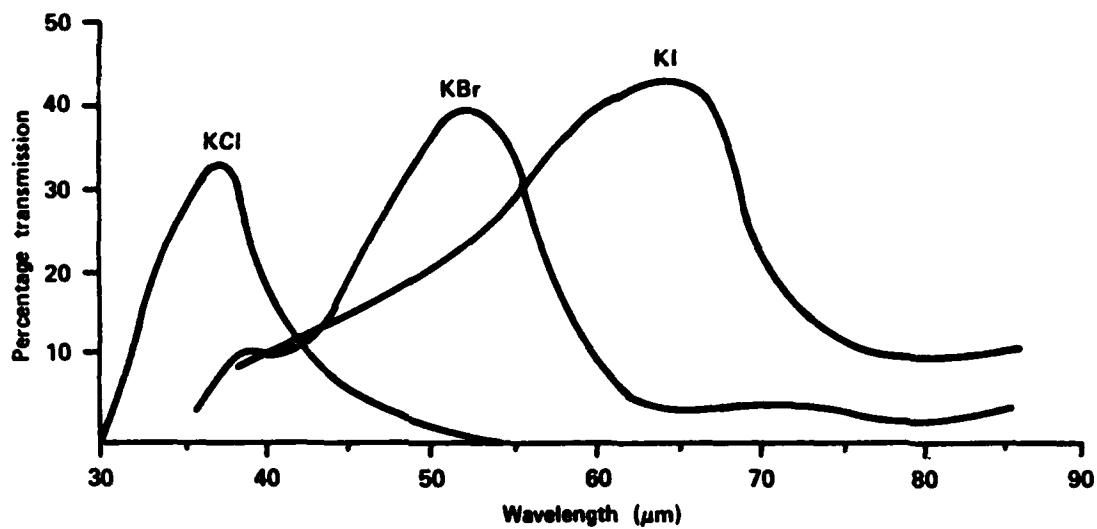


Figure 4. Curves Showing the Christiansen Transmission Peaks for Powdered KCl, KBr, and KI.<sup>10</sup>

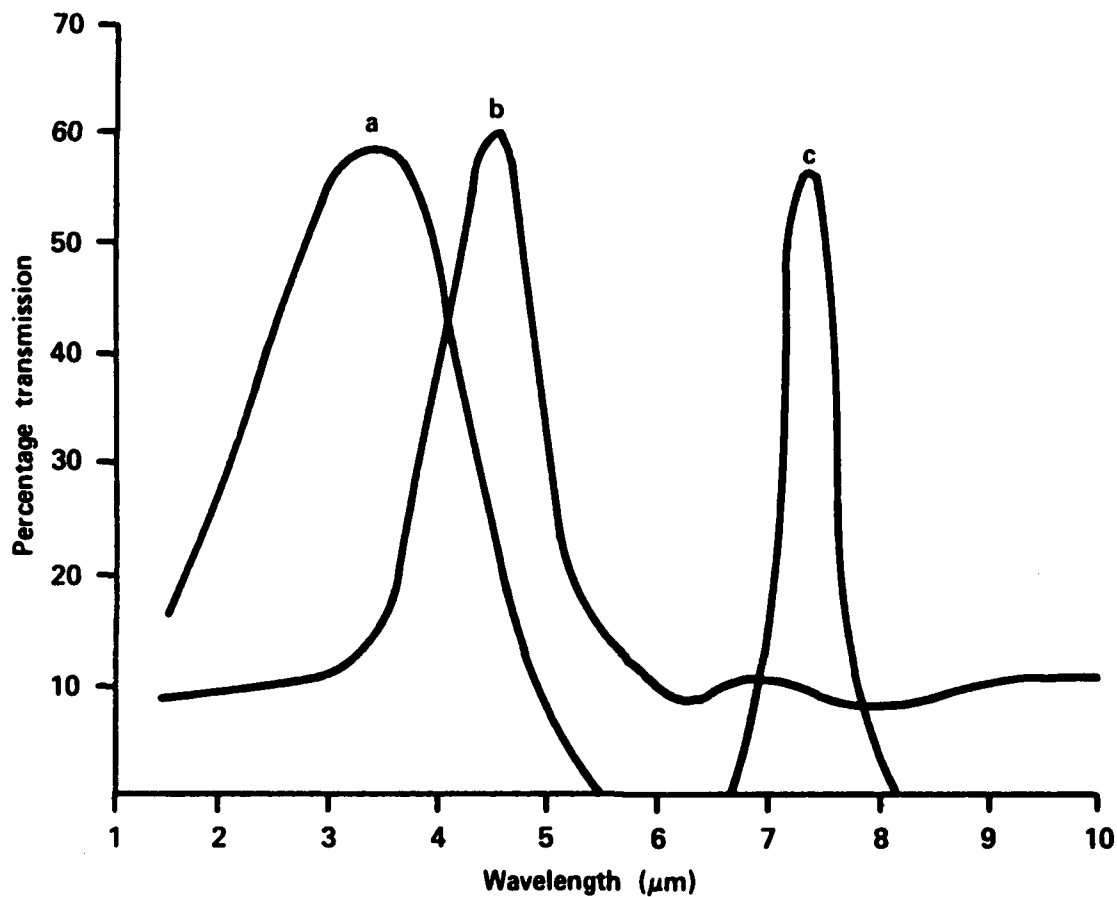


Figure 5. Shift of the Christiansen Peak for Quartz Powder in Liquids. (a) Quartz in a 50% by Volume Mixture of  $\text{CS}_2$  and  $\text{CCl}_4$ ; (b) Quartz in Pure  $\text{CCl}_4$ ; (c) Quartz in Air.

Sethill has published an equation that is stated to give a good approximation to the transmittance at a Christiansen wavelength:

$$T_{\lambda} = 1/2 [\exp(-k_{L_{\lambda}} X t) + \exp(-k^1_{L_{\lambda}} X t)] \times \exp \left[ -7tD_{\mu} \left( \frac{n_{\lambda} - 1}{\lambda} \right)^2 \right] \quad (1)$$

In effect, this equation predicts a transmittance that is the product of the averaged energy not absorbed during transmission of the ordinary and extraordinary rays, times an empirical relationship for energy not scattered by the particles.

### 3. EXPERIMENTAL PROCEDURES

It is desired to determine whether the Christiansen effect observed in the laboratory for silica dust films on substrates could be duplicated in actual soil-derived, predominately silica dust clouds in the atmosphere. A sample of sandy topsoil, typical of the alluvial soils found near the Chesapeake Bay, was dug at Edgewood, Maryland. The sample was dried and placed without further preparation into a 0.95-liter (1-qt) glass jar with a metal screw cap. The capped jar was wrapped with explosive primacord and placed in an explosive test chamber having an optical path length between diametrically opposed viewpoints of  $L = 6\text{m}$ . An IR radiometer and instrumentation described earlier<sup>3</sup> were used with the chamber.

The explosive was detonated, resulting in a dust cloud containing a large fraction of particles distributed broadly<sup>6</sup> over the range of particle sizes included in Figure 2. The upper (solid) curve in Figure 6, which was corrected for water vapor in the chamber, was taken when the airborne mass dust concentration was  $C = 0.24 \text{ g/m}^3$ . The equation for a homogeneous film precipitated from an aerosol is<sup>3</sup>

$$t = (C \times L)/p \quad (2)$$

Since  $p = 2.66 \text{ g/cm}^3$  for silica, the equivalent film thickness for this spectrum was  $t = (0.24 \times 6)/2.66 = 0.54 \text{ } \mu\text{m}$ .

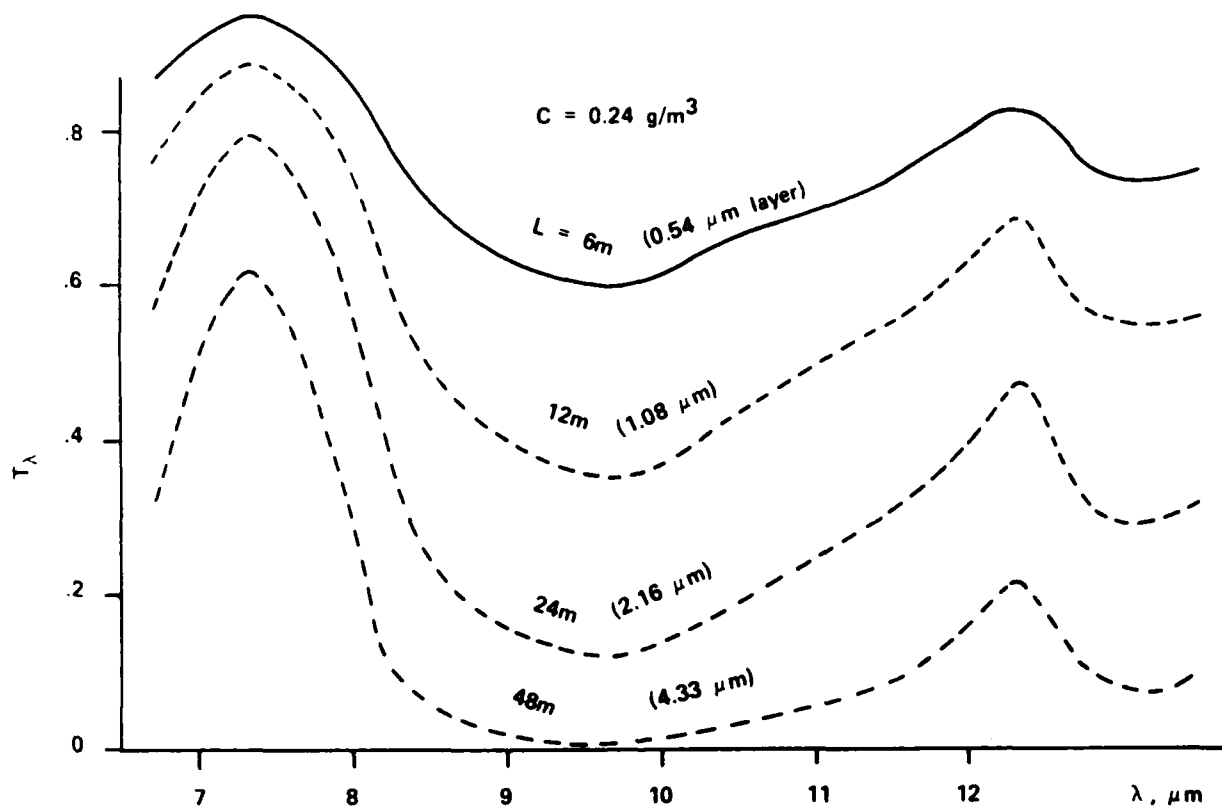


Figure 6. Measured IR Spectrum of an Experimental Dust Cloud (Upper, Solid Curve) and Calculated Spectra (Dashed Curves) for Longer Optical Path Lengths or Cloud Depths. Each Curve is Labeled with the Actual or Calculated Path Length  $L$  in Meters and the Equivalent Dust Film Thickness for a Precipitated Layer in Micrometers.

The Beer-Lambert law for aerosols is

$$\ln(1/T_\lambda) = \alpha_\lambda CL. \quad (3)$$

The peak IR extinction coefficient for this test cloud was observed near  $\lambda = 9.8 \mu\text{m}$  as  $\alpha_{9.8} = 0.35 \text{ m}^2/\text{g}$ . A He-Ne laser, operating concurrently in the visible, indicated an extinction coefficient of  $\alpha_{0.63} = 0.49 \text{ m}^2/\text{g}$ . Using Equation (3) and the measured spectrum (solid curve) from Figure 6, wavelength-by-wavelength calculations were then made for progressively greater cloud thicknesses, or optical path lengths, of  $L = 12 \text{ m}$ ,  $24 \text{ m}$ , and  $48 \text{ m}$ . The calculated spectra are shown with their  $L$  values by the dashed curves in Figure 6, which also shows the equivalent film thicknesses,  $t = 1.08 \mu\text{m}$ ,  $2.16 \mu\text{m}$ , and  $4.33 \mu\text{m}$ , respectively, from Equation (2) for each calculated cloud.

When the lower dashed curve in Figure 6 is compared to the dashed curve of Henry in Figure 3, for an equivalent thickness  $t = 4.1 \mu\text{m}$ , very good agreement is seen. In Figure 6 for an experimentally derived and calculated solid dust cloud  $48 \text{ m}$  thick and containing an equivalent  $4.33 \mu\text{m}$  of precipitable dust, the peak transmittance at  $\lambda = 7.4 \mu\text{m}$  was about  $0.6$  with a secondary peak of  $T_\lambda = 0.2$  beyond  $12 \mu\text{m}$ . Thus, the data seem to indicate that the silica (quartz) samples for Henry's filters and those for the experimental dust cloud were very similar in their Christiansen effect and, furthermore, that their respective particle diameters were roughly equivalent. Such agreement may, however, be fortuitous for the experimental soil samples used from the Chesapeake Bay area. No inference should be drawn that sandy soils from diverse geographical locations will give such apparently clear-cut evidence of Christiansen behavior.

#### 4. DISCUSSION

From Figure 2, it is straightforward to show that the shape of the shortwavelength side of the  $7.4 \mu\text{m}$  silica-air optical passband is determined by optical scattering, while the shape of the longwavelength side is determined by absorption of the silica particles. For the particle size of  $15.5 \mu\text{m}$ , the passband in Figure 2 (solid curve) is cleanly defined. With the layer thickness held constant at  $t = 12.8 \mu\text{m}$ , transmission of the shortwavelength side of the passband increases as the particle diameter is reduced to  $D_\mu = 6.6 \mu\text{m}$ , i.e., as the particle size becomes smaller compared to the wavelength of the Christiansen peak,  $\lambda = 7.45 \mu\text{m}$ . When the particle diameter is reduced still further to  $D_\mu = 1.0 \mu\text{m}$ , i.e., when  $D_\mu \ll \lambda$ , extinction due to scattering on the shortwavelength side of the passband is greatly reduced, and the filter characteristic is largely destroyed. Similar effects can be seen at longer wavelengths (beyond  $10 \mu\text{m}$ ) in Figure 2.

In the latter case, a Rayleighlike scattering situation exists.<sup>3,12</sup> That is, the particles have become so small compared to the wavelength of interest (7.4  $\mu\text{m}$ ) that their scattering contribution to the total optical extinction coefficient  $\alpha_{7.4}$  has become nearly negligible compared to their absorption. It has been shown in Section 3 that a cloud of silica dust in air has a spectrum like that of a precipitated film of silica dust on a substrate, i.e., the spectra of Figures 3 and 6 are similar. When a silica dust cloud exists in the (moist) atmosphere, however, the loss of scattering extinction of the shortwavelength side of the passband is offset by absorption of the shoulder of the  $\nu_2$  band of water vapor, which is centered at  $\lambda = 6.3 \mu\text{m}$ . Thus, the spectrum of a 7.4  $\mu\text{m}$  Christiansen filter formed by a silica dust cloud in the atmosphere would combine with the water vapor spectrum to give a well-defined passband determined by water absorption on the shortwavelength side and dust particles absorption on the longwavelength side, over wide ranges of dust particle size distributions and water vapor concentrations. Absorption by the longer-wavelength shoulder of the 6.3  $\mu\text{m}$  water vapor band becomes significant as the atmosphere path length is increased.

Consider a silica dust cloud 48 m thick, like the one represented by the lower dashed spectrum of Figure 6, existing in the moist atmosphere at 20 °C and 50% RH. The transmittances of the water vapor in a 48 m optical path under these conditions are 0.66 at  $\lambda = 7.0 \mu\text{m}$ , 0.92 at 7.4  $\mu\text{m}$ , and 0.99 at 8.0  $\mu\text{m}$ . Thus, even through an atmospheric path of only 48 m, water vapor absorption would begin to shape the shortwavelength side of the Christiansen dust passband centered at 7.4  $\mu\text{m}$ . For longer optical paths, atmospheric transmission in the 7-8  $\mu\text{m}$  region rapidly diminishes due to water vapor absorption. For example, 1 km of moist air at 20 °C and 50% RH has a transmittance of 0.0002 at  $\lambda = 7.0 \mu\text{m}$ , 0.18 at 7.4  $\mu\text{m}$ , and 0.77 at 8.0  $\mu\text{m}$ . Thus, in any potential application, the combined effects of dust clouds and atmospheric gases, especially water vapor, must be considered in determining the effective shape of the optical passband centered on the Christiansen wavelength.

At the Christiansen wavelength, the real refractive indices of, for example, a silica dust cloud or film and air, become equal, and the medium becomes homogeneous so that optical transmittance is limited only by particle absorption. In Equation (1), for example, when  $n_{7.4} \approx 1.0$ , the transmittance at 7.4  $\mu\text{m}$  is limited only by the average absorption of all rays. These conditions are similar to Rayleighlike scattering conditions of droplet aerosols,<sup>3,12</sup> for which useful approximations apply, for example (see the Appendix),

$$k_{L\lambda} \approx \alpha_{\lambda} X p \quad (4)$$

(at Christiansen wavelength), where the precision of the

approximation is discussed in Reference 12. Since by definition  $k_{L\lambda} = 4 \pi k_{\lambda} / \lambda$ , it follows that

$$\frac{4\pi k_{\lambda}}{\lambda} \approx \alpha_{\lambda} \times p \quad (5)$$

(at Christiansen wavelength) or

$$k_{\lambda} \approx \frac{\alpha_{\lambda} \times p \times \lambda}{4\pi} \quad (6)$$

(at Christiansen wavelength). That is, at the wavelength of peak transmission by the Christiansen passband, the imaginary index of the particles may be approximated by Equation 6. As an example, consider a silica dust cloud spectrum, shown as the lower dashed curve in Figure 6, where, in Equation 3,  $T_{7.4} = 0.62$ ,  $C = 0.24 \text{ g/m}^3$ , and  $L = 48 \text{ m}$ , so that  $\alpha_{7.4} = 0.04 \text{ m}^2/\text{g}$ . If  $p = 2.66 \text{ g/cm}^3$  for silica, from Equation 6 for  $\lambda = 7.4 \text{ } \mu\text{m}$ ,  $k_{7.4} = (0.04) (2.66) (7.4) / 4\pi = 0.065$ .

At this wavelength, Equation 3 can be rewritten using Equations 2 and 4 as follows:

$$\ln(1/T_{\lambda}) = k_{L\lambda} \times t \quad (7)$$

(at the Christiansen wavelength), which is the equivalent expression for an absorbing, precipitated film. No representation is made that Equations 4 - 7 are more than useful approximations, because they are based upon spherical or near-spherical particles subject to considerations including those discussed above. But these equations are found to be quite useful, and, more importantly, they clarify the relationships between particulate clouds and precipitated films that exhibit the Christiansen effect and more conventional aerosols.

Table 1 and Figure 4 show the Christiansen wavelengths for various materials in air, including several common salts. In theory, spectra taken over long optical paths in atmospheres containing dry salt (maritime) condensation nuclei should tend to show enhanced transmission near their corresponding Christiansen wavelengths.

Middleton<sup>13</sup> defines "meteorological range" as that range for a high-contrast target (e.g., an illuminated hole in a black box viewed by the eye) where the transmittance reaches  $T_{\lambda} = 0.02$ . From Equation 3, this corresponds to the case for  $\alpha_{\lambda} CL = 3.912$ . For the examples used in this report (moist air at

20 °C, 50% RH, and a dust cloud for which  $C = 0.24 \text{ g/m}^3$  as for the lower curve of Figure 6), this range would be 345 m at  $\lambda = 7.4 \text{ }\mu\text{m}$ , the Christiansen peak. At this wavelength, 15% of the optical extinction would be due to water vapor absorption, and 85% would be due to absorption of the silica particles in the cloud.

## 5. CONCLUSIONS

The primary conclusion to be drawn from this work is that Christiansen effects can occur in dust or particulate clouds in the atmosphere, and that their possible implications should be considered by atmospheric physicists and IR systems designers. By comparative study (the theory and literature of powder film, Christiansen filters on optical substrates, and new measurements of dust cloud spectra), it has been shown that aerosols, including those exhibiting the Christiansen effect, can be represented by equivalent precipitated, homogeneous films under many conditions. These observations allow simple approximation equations to be derived that are generally useful in aerosol spectroscopy.

## LITERATURE CITED

1. Christiansen, C., Ann. Phys. (Leipzig) Vol. 23, p 298 (1884).
2. Christiansen, C., Ann. Phys. (Leipzig) Vol. 24, p 439 (1885).
3. Carlon, H.R., Anderson, D. H., Milham, M. E., Tarnove, T. L., Frickel, R. H., and Sindoni, I., "IR Extinction Spectra of Some Common Liquid Aerosols," Appl. Opt. Vol. 16, p 1598 (1977).
4. Carlon, H. R., Appl. Opt. Vol. 1, p 603 (1962).
5. Reichert, C. C., Jr., The Christiansen Optical Dispersion Filter: A Bibliography, EASP 300-3, Defense Development and Engineering Laboratories, Edgewood Arsenal, MD, December 1968 UNCLASSIFIED Report. (AD 846 631)
6. Carlon, H. R., "Mass Extinction Coefficients (0.55  $\mu$ m - 14  $\mu$ m) of Soil-Derived Atmospheric Dusts," Appl. Opt. (1979).
7. Smith, R. A., Jones, F. E., and Chasmar, R. P., The Detection and Measurement of Infrared Radiation, Clarendon Press, Oxford, London, p 396, 1968.
8. Henry, R. L., J. Opt. Soc. Am. Vol. 38, p 775 (1948).
9. Spitzer, W. G. and Kleiman, D. A., J. Appl. Phys. Vol. 121, p 1324 (1961).
10. Barnes, R. B. and Bonner, L. G., J. Appl. Phys. Rev. Vol. 49, p 732 (1936).
11. Sethi, N. K., Indian J. PHYS. Vol. 6, p 121 (1921).
12. Carlon, H. R., "Practical Upper Limits of the Optical Extinction Coefficients of Aerosols," Appl. Opt. Vol. 18, p 1372 (1979).
13. Middleton, W. E. K., Vision Through The Atmosphere Univ. Toronto Press, Toronto, p 105, 1952.

Blank

APPENDIX  
ADDITIONAL OBSERVATIONS

Blank

## APPENDIX

### ADDITIONAL OBSERVATIONS

In this report, it was stated that at a Christiansen wavelength,  $\lambda$ , Rayleighlike scattering conditions exist that are similar to those for droplet aerosols for which useful approximations apply, e.g.,

$$\alpha_{\lambda} \cdot p \approx k_{L\lambda} \tag{1}$$

where  $k_L$  is the absorption coefficient of an equivalent precipitated film ( $\mu\text{m}^{-1}$ ),  $\alpha$  is the optical extinction coefficient of the aerosol ( $\text{m}^2/\text{g}$ ), and  $p$  is the particle mass density ( $\text{g}/\text{cm}^3$ ). The purpose of this appendix is to discuss in greater detail the scattering at the Christiansen wavelength and to develop mathematical approximations for this special case.

The precision of Approximation (1) is discussed in Reference 1, where for spherical droplets or particles of diameter  $D_{\mu}$  ( $\mu\text{m}$ ) a small-particle limit exists for the Rayleigh regime so that

$$\alpha_{\lambda} \cdot p = k_{L\lambda} \cdot f(m_{\lambda}), \tag{2}$$

where

$$f(m_{\lambda}) = \left[ \frac{9n}{(n^2+k^2)^2 + 4(n^2-k^2) + 4} \right]_{\lambda} \tag{3}$$

and  $n_{\lambda}$  and  $k_{\lambda}$  are the real and imaginary parts of the refractive index. But for the Christiansen wavelength in air,  $n_{\lambda} \approx 1.0$ , so that

$$\alpha_{\lambda} \cdot p = k_{L\lambda} \left[ \frac{9(1)}{(1+k^2)^2 + 4(1-k^2) + 4} \right]_{\lambda} \tag{4}$$

and since<sup>1</sup>

$$k_{L\lambda} = (4\pi k_{\lambda})/\lambda, \tag{5}$$

<sup>1</sup>H.R. Carlon, App. Opt. 18,1372 (1979).

it is straightforward to show that the aerosol extinction coefficient in the Rayleigh limit becomes

$$a_{\lambda} = \frac{36\pi k_{\lambda}}{\lambda \cdot p(9-2k_{\lambda}^2 + k_{\lambda}^4)} \quad (6)$$

for the Christiansen wavelength ( $n_{\lambda} = 1.0$ ).

For small values of  $k_{\lambda} (< 1.0)$ , the term  $k_{\lambda}^4$  in Equation 6 is small, and an approximation equation can be written:

$$a_{\lambda} \approx \frac{36\pi}{\lambda \cdot p (9/k_{\lambda} - 2k_{\lambda})} \quad (7)$$

for the Christiansen wavelength ( $n_{\lambda} = 1.0$  and  $k_{\lambda} < 1.0$ ).

A sensitivity analysis reveals that (7) yields approximations to within  $\approx 10\%$  of the values of Equation 6 when  $k_{\lambda} \leq 0.92$ , a condition that is fulfilled for most substances comprising spherical-particle aerosols.

Mie<sup>2</sup> calculations can be performed for spherical particles at the Christiansen wavelength ( $n_{\lambda} = 1.0$ ), and the results can be plotted as in Figure A-1 for the normalized extinction coefficient  $a_{\lambda} \cdot \lambda \cdot p$  vs. size parameter  $\pi D_{\mu} / \lambda$ . In Figure A-1,  $k_{\lambda}$  is taken as 1.00. In the small-particle (Rayleigh) limit where the size parameter is less than 1, the absorption and extinction curves merge, showing that virtually all extinction arises from absorption. The curves level at  $a_{\lambda} \cdot \lambda \cdot p = 13$  or 14, which agrees with the value of 14 obtained from Equation 6 when  $k_{\lambda} = 1.0$ . The error in approximation (7) is  $\sim 14\%$  at  $k_{\lambda} = 1.0$ , and thus this equation produces a value of  $a_{\lambda} \cdot \lambda \cdot p = 16$  for these conditions. It can also be seen in Figure A-1 that the solid extinction curve is very smooth to the Mie region ( $D_{\mu} \approx \lambda / \pi$ ). This is typical of absorbing aerosols and contrasts with the pronounced peak here for predominantly scattering aerosols, usually accompanied by ripples of diminishing magnitude toward larger size parameters.

An interesting example of application of (7) is that of the silica Christiansen wavelength at  $\lambda = 7.4 \mu\text{m}$ , from which  $k_{7.4} \approx 0.065$  so that

<sup>2</sup>G. Mie, Ann. Phys. 25, 377 (1908).

$$\alpha_{7.4} = \frac{36\pi}{(7.4)(2.66)[9/0.65^{-2}(.065)]} \quad (8)$$
$$\approx 0.042 \text{ m}^2/\text{g}$$

where  $\alpha_{7.4}$  is entirely due to particle absorption and corresponds to the region of merging and flattening of the absorption and extinction curves in Figure A-1 for the example given there. By comparison,  $\alpha_{\lambda}$  at nearby wavelengths where the Christiansen effect does not occur and scattering contributes to extinction can be much larger, e.g.,  $\alpha_{9.6} \approx 0.33 \text{ m}^2/\text{g}$ .

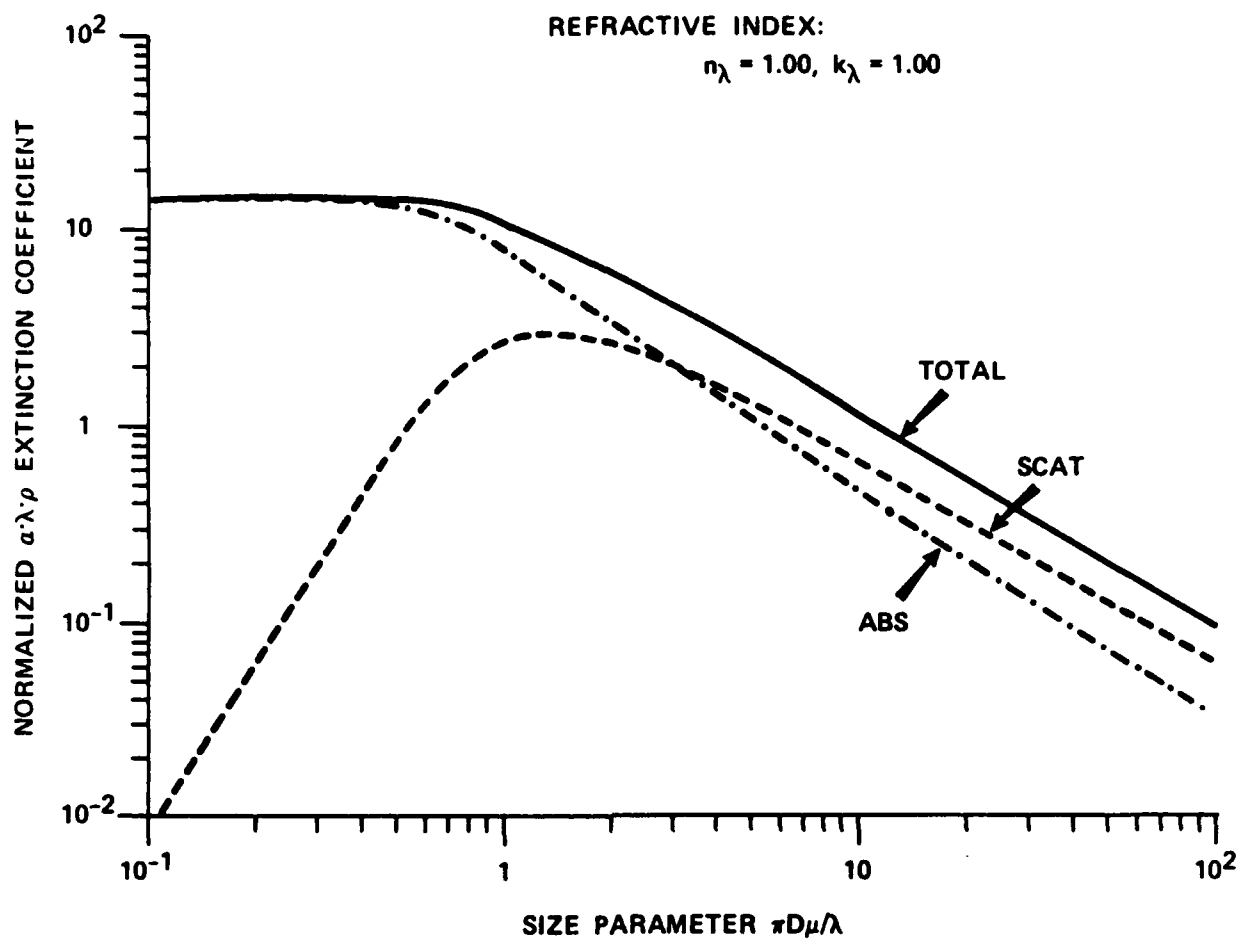


Figure A-1. Normalized Extinction Coefficient vs. Size Parameter for Spherical Aerosol Particles at the Christiansen Wavelength  $\lambda$ , Where  $n_\lambda = 1.00$  and  $k_\lambda = 1.00$ .

END

FEB.

1988

DTIC